Journal of Computational Mathematics, Vol.11, No.2, 1993, 113–128.

A RANDOM NUMERICAL METHOD WITH APPLICATION IN COMBUSTION*

Yu Song

(Department of Mathematics, Tulane University, New Orleans, USA)

Abstract

This paper presents a random numerical method which combines the random vortex method and the random choice method. A random choice method is used for the modeling reaction-diffusion system. The splitting of source terms in two dimensions for the random choice method is tested. A hybrid random vortex method is used for solving the Navier-Stokes equation which governs the fluid motion. With the assumption of incompressibility, the fluid motion can be uncoupled from the chemistry. The method is applied to a flow passing a circular cylinder which is kept cold or heated. In both cases the method demonstrates an ability to resolve turbulent effects on flame front propagation.

§1. Introduction

A. Equations of Fluid Motion

Consider a two-dimensional Navier-Stokes equation in a domain D with boundary ∂D:

$$\begin{aligned} &\partial_t \boldsymbol{u} + (\boldsymbol{u}\cdot\nabla)\boldsymbol{u} = Re^{-1}\triangle \boldsymbol{u} - \frac{\nabla P}{\rho}, && \text{in } D,\\ &\operatorname{div}(\boldsymbol{u}) = 0, && \text{in } D,\\ &\boldsymbol{u} = (0,0), && \text{on } \partial D \end{aligned} \tag{1.1}$$

where $\boldsymbol{u} = (u, v)$ is the velocity vector, $\boldsymbol{r} = (x, y)$ is the position vector, t is time, $\triangle \equiv \nabla^2$ is the Laplacian operator, P is pressure, ρ is density and Re is the Reynolds number associated with flow.

Equation (1.1) is difficult to solve by a finite-difference method, particularly at large Reynolds numbers. Chorin ([5], [8]) has developed a grid-free method for modeling turbulent flow. In that method, the random vortex method, the creation of vorticity along boundaries is modeled by creation of vortex blobs, discrete quantities of vorticity. The vortex blobs themselves are not vortices but elements whose unions form vortices. The motion of the fluid flow is modeled by considering the interaction of these blobs. The random vortex method and vortex sheet method are described in Section 2.

* Received August 1, 1990.

B. Equations of Combustion

Combustion is governed by a complicated interaction of advection, diffusion and reaction. For simplicity, we consider a single step reaction given by $A \rightarrow B$ which describes a premixed combustible or an oxidation reaction where either fuel or oxidizer is present in small quantities. When written in dimensionless variables, the equations governing this combustion process are

$$\rho(\partial_t Y_A + (\boldsymbol{u} \cdot \nabla) Y_A) = Le_A^{-1} \triangle Y_A - \rho K_A Y_A e^{-N_A/T},$$

$$\rho(\partial_t T + (\boldsymbol{u} \cdot \nabla) T) = \triangle T + \rho Q_A K_A Y_A e^{-N_A/T} \tag{1.2}$$

where T is temperature, ρ is density, Y_A is mass fraction of chemical spices A, $\boldsymbol{u}$ is the velocity vector of fluid flow, Le_A is the Lewis number associated with the mixture and Q_A is the heat released by the reaction. The reaction rate is determined by N_A, the activation energy, and K_A, the pre-exponential factor. In this form, $0 \leq Y_A \leq 1$ and in absence of external heat $T_u \leq T \leq T_b + \varepsilon$ with $T_b = 1 + T_u$, where T_u is ambient temperature, T_b is burning temperature, ϵ is to accommodate slight overshoot of T possible for a reaction which is much faster than diffusion.

To solve equation (1.2) numerically, difficulties arise due to the difference in time scales, especially in a fast reaction. A very small time step is necessary in order to maintain the stability of the solution (Dwyer and Otey[11]). The random choice method of Glimm[12] has successfully modeled the system of hyperbolic conservation laws (Chorin[6], Sod[19]) and is suitable for solving differential equations which have steep gradients in the solution profiles. Sod[22] has shown how the random choice method can be extended to solve reaction-diffusion equations. The applications of the method can be found in Sod [23] [24].

We combine a hybrid vortex method with the random choice method to model the turbulent combustion phenomina. The combustion model is applied to the ignition of a flow pussing a circular cylinder. The flow produces vortices behind the cylinder; the flame profiles show that the correct modeling of vortices is important as propagation of the flame.

§2. Vortex Methods

A. The Random Vortex Method

We introduce the vorticity $\xi = \nabla \times \boldsymbol{u} = \partial_x v - \partial_y u$. By taking the curl ($\nabla\times$) of equation (1.1), we obtain the scalar vorticity transport equation

$$\partial_t \xi + (\boldsymbol{u} \cdot \nabla)\xi = Re^{-1} \triangle \xi, \quad \text{div}\,(\boldsymbol{u}) = 0. \tag{2.1}$$

The vorticity field ξ gives rise to a velocity field u which transports it. A stream function ψ is introduced which satisfies

$$u = \partial_y \psi, \quad v = -\partial_x \psi. \tag{2.2}$$

Using the definition of vorticity, we obtain a relationship between ψ and ξ:

$$\triangle\psi = -\xi, \quad \text{in } D.$$

The vortex method is based upon this stream function-vorticity formulation. The construction of the vortex blob method consists of four steps:

Step1. First assume the flow is inviscid, that is, $R_e^-1 = 0$ and there are no boundaries. Equation (2.1) reduces to the inviscid Euler equations

$$D\xi/Dt = 0, \quad \triangle\psi = -\xi \tag{2.3}$$

where D/Dt denotes the total derivative. Consider a collection of N point vortices with circulations $\xi_1, \xi_2, \cdots, \xi_N$ located at points $\boldsymbol{r}_1, \boldsymbol{r}_2, \cdots, \boldsymbol{r}_N$ respectively and total vorticity is $\xi = \sum_{j=1}^{N} \xi_j$. We may write the vorticity field in the form

$$\xi(\boldsymbol{r}) = \sum_{i=1}^{N} \xi_i \xi_0(\boldsymbol{r} - \boldsymbol{r}_i), \tag{2.4}$$

where $\xi_0(\boldsymbol{r})$ is an approximation of Dirac delta function $\delta(\boldsymbol{r})$ proposed by Chorin [5]:

$$\xi_0(\boldsymbol{r}) = \begin{cases} \dfrac{1}{2\pi\sigma\|\boldsymbol{r}\|} & \|\boldsymbol{r}\| < \sigma, \\ 0, & \|\boldsymbol{r}\| \geq \sigma; \end{cases} \tag{2.5}$$

here σ is a cut-off value to be determined later.

Solving the stream function, we have

$$\psi_0(\boldsymbol{r}) = \begin{cases} -\dfrac{1}{2\pi\sigma}\|\boldsymbol{r}\| + \text{ constant}, & \|\boldsymbol{r}\| < \sigma, \\ -\dfrac{1}{2\pi}\ln\|\boldsymbol{r}\|, & \|\boldsymbol{r}\| \geq \sigma. \end{cases} \tag{2.6}$$

The velocity field from (2.2) is

$$u_0(\boldsymbol{r}) = \begin{cases} \left(\dfrac{-y}{2\pi\sigma\|\boldsymbol{r}\|}, \dfrac{x}{2\pi\sigma\|\boldsymbol{r}\|}\right), & \|\boldsymbol{r}\| < \sigma, \\ \left(\dfrac{-y}{2\pi\|\boldsymbol{r}\|^2}, \dfrac{x}{2\pi\|\boldsymbol{r}\|^2}\right), & \|\boldsymbol{r}\| \geq \sigma. \end{cases} \tag{2.7}$$

The velocity field induced by the vorticity field $\xi(\boldsymbol{r})$ in (2.4) is

$$\boldsymbol{u}(\boldsymbol{r}) = \sum_{i=1}^{N} \xi_i \boldsymbol{u}_0(\boldsymbol{r} - \boldsymbol{r}_i), \tag{2.8}$$

Step 2. Consider the normal boundary condition $\boldsymbol{u} \cdot \boldsymbol{n} = 0$ where n is an outward pointing unit normal to ∂D. This condition is satisfied by adding a potential flow to the flow field induced by the vorticity field.

Step 3. Neglect the boundary and consider $R_e^-1 \neq 0$. Consider the diffusion equation

$$\partial_t \xi = Re^{-1} \triangle \xi.$$

In this, viscosity is included by adding a random walk component to the discrete solution of the Euler's equation.

Step 4. We reintroduce the boundaries and consider the tangential boundary condition:

$$\boldsymbol{u} \cdot \boldsymbol{s} = 0, \quad \text{on } \partial D \tag{2.9}$$

where $\boldsymbol{u} = \boldsymbol{u}_\xi + \boldsymbol{u}_P$ from Steps 1 and 2, and $\boldsymbol{s}$ is the unit vector in tangential direction. Simulating the way in which the vorticity is created in flows,Chorin [5] proposed a vorticity creation algorithm on ∂D. Vortex blobs are introduced at points on ∂D, equally spaced a distance $\triangle h$ apart, with vorticity $\boldsymbol{u} \cdot \triangle h$ so that the induced velocity as the vortex blob moves of ∂D will satisfy $\boldsymbol{u} \cdot \boldsymbol{s} = 0$.

Combining the previous steps, the discrete approximation is

$$\begin{aligned} x_i^{n+1} &= x_i^n + \triangle t(u_i + u_{pi}) + \eta_{i1}, \\ y_i^{n+1} &= y_i^n + \triangle t(v_i + v_{pi}) + \eta_{i1}, \end{aligned} \tag{2.10}$$

where (u_i, v_i) is from Step 1 in (2.8) and (u_{pi}, v_{pi}) potential flow ftom Step 2. (η_1, η_2) is an independent Gaussian random variable with mean 0 and variance $2\Delta t/R_e$.

B. Vortex Sheet Method

The rate of convergence near ∂D is slow with the method of vorticity creation presented above. Chorin [8] introduced a new vorticity generation technique, the vortex sheet method, based on the fact that, within the boundary layer, the Navier-Stokes equation can be approximated by the Prandtl equation (Schlichting [18]):

$$\partial_t \xi + (\boldsymbol{u} \cdot \nabla)\xi = Re^{-1}\partial_y^2 \xi, \tag{2.11a}$$

$$\xi = -\partial_y u, \tag{2.11b}$$

$$\operatorname{div}(\boldsymbol{u}) = 0, \tag{2.11c}$$

where $\boldsymbol{u} = (u, v)$, u is tangential to ∂D and v is normal to ∂D. Computational element vortex sheet S_i is tangential to the boundary of length $\triangle h$ and centered at $\boldsymbol{r}_i = (x_i, y_i)$.

The intensity ξ_i of vortex sheet is defined such as

$$\xi_i = -(u(y_i^+) - u(y_i^-)),$$

the jump of the velocity as y crosses the vortex sheet S_i. Equation (2.11b) can be integrated in the form

$$u(x, y) = U_\infty(x) - \int_y^\infty \xi(x, \tau)d\tau \tag{2.12a}$$

and equation (2.11c) yields

$$v(x, y) = -\partial_x \int_0^y \xi(x, \tau)d\tau. \tag{2.12b}$$

It can be readily seen that if ξ is known, $\boldsymbol{u} = (u, v)$ can be calculated by (2.12).

Consider a collection of N segments S_i of vortex sheets of intensities ξ_i and centered $r_i, i = 1, \cdots, N$. The velocity $u_i = (u_i, v_i)$ of S_i is obtained by discretizing (2.12):

$$u_i = U_\infty(x_i) - \frac{1}{2}\xi_i - \sum_{j \neq i} \xi_j d_j \tag{2.13}$$

where $d_j = 1 - \dfrac{|x_j - x_i|}{\triangle h}$ and the summation is taken over all j such that $y_j^n > y_i^n$ and $d_j > 0$.

$$v_i = -(I_+ - I_-)/\triangle h \tag{2.14}$$

where

$$I_\pm = U_\infty(x_i) - \Sigma_\pm \xi_j d_j^\pm y_j^*,$$

$$d_j^\pm = 1 - |x_i \pm \frac{\triangle h}{2} - x_j|/\triangle h,$$

$$y_j^* = \min(y_i, y_j).$$

The sum Σ_+ (resp. Σ_-) is over S_j such that $d_j^+ \leq 1$ (resp. $d_j^- \leq 1$).
From (2.13) and (2.14), the position of the vortex sheets are moved according to

$$x_i^{n+1} = x_i^n + \Delta t u_i, \quad y_i^{n+1} = y_i^n + \Delta t v_i + \eta_i$$

where σ_i is a Gaussian distribution with mean 0 and variance $2 \triangle t/R_e$, which only applies to y-component since diffusion in the x-direction is neglected on the Prandtl boundary layer approximation.

§3. The Random Choice Method

A. The Random Choice Method for a Reaction-Diffusion System

Consider the reaction-diffusion system of equations

$$\partial_t V + \partial_x F(V) = \bar{v}\partial_x^2 V + G(V), \quad V(x,0) = f(x) \tag{3.1}$$

where $\boldsymbol{v} = (v_1, v_2, \cdots, v_p), \bar{v} = \text{diag}\ (v_1, v_2, \cdots, v_p)$, with $v_i \geq 0$, $i = 1, \cdots, p$, $\boldsymbol{G}$ is a nonlinear reaction or source term and the Jacobian of F, $\partial F_i/\partial v_i$ has real and distinct eignvalues.

If $\bar{v} = 0$ and $\boldsymbol{G} = 0$, (3.1) reduces to a system of hyperbolic conservation laws:

$$\partial_t \boldsymbol{v} + \partial_x \boldsymbol{F}(\boldsymbol{v}) = 0. \tag{3.2}$$

A random choice scheme was proposed by Glimm [12] to construct solutions to (3.2) and prove existence under the condition that the total variation of the initial data is sufficiently small. The method was developed as a computational technique by Chorin([6], [7]), Colella([10]) and Sod ([19], [21]). For the numerical solution of (3.1), the general flow can be decomposed into elementary waves (3.2) and steady

waves (Sod[22]), as in the method developed by Liu([14][15]) using a boundary value problem to obtain the steady waves. The steady waves reduce to the system of ordinary differential equtions

$$\partial_x \boldsymbol{F}(\boldsymbol{v}) = \bar{\nu}\partial_x^2 \boldsymbol{v} + \boldsymbol{G}(\boldsymbol{v}). \tag{3.3}$$

Given the approximate solution $\boldsymbol{u}_i^n$ to $\boldsymbol{v}(ih, ik)$, where h is the space step size and k is the time step length. Firstly, (3.3) is solved as a two-point boundary value problem in each interval $[ih, (i+1)h]$ to obtain a steady state solution v^s with boundary conditions

$$\boldsymbol{v}^s(ih) = \boldsymbol{u}_i^n, \quad \boldsymbol{v}^s((i+1)h) = \boldsymbol{u}_{i+1}^n. \tag{3.4}$$

The solution on $[ih, (i+1)h]$ is sampled at the midpoint to produce a piecewise constant approximation

$$\boldsymbol{v}(x, nk) = \boldsymbol{u}_{i+1/2}^n = \boldsymbol{v}^s((i+1/2)h), \quad ih < x < (i+1)h.$$

The conservation laws (3.2) are solved using Glimm's method for $nk \le t \le (n+1)k$, with the piecewise constant states as initial conditions

$$\boldsymbol{v}(x, nk) = \boldsymbol{u}_{i+1/2}^n, \quad ih < x < (i+1) \cdot h.$$

Thus, a sequence of Riemann problems is produced centered at the grid points $x = ih$. If the CFL condition is satisfied, that is, $h/k = \dfrac{1}{2\lambda_i(\boldsymbol{v})}$, for all eigenvalues λ_i, $i = 1, 2, \cdots, p$, of Jacobian of $\boldsymbol{F}(\boldsymbol{v})$, the waves generated by the individual Riemann problem will not interact. Hence, each is solved separately and the solutions can be combined by superposition into a single exact solution , denoted by $\boldsymbol{v}^e(x, t)$ defined for $nk \le t \le (n+1)k$. Define the approximate solution for (3.1) at the next time level by

$$\boldsymbol{u}_i^{n+1} = \boldsymbol{v}^e((i+\xi_n)h, (n+1)k)$$

where ξ_n is an equidistributed random variable in the interval (-1/2, 1/2).

By applying the random walk solution to the diffusion equation, Sod [22] showed that for a single scalar coefficient equation

$$\partial_t v + c\partial_x v = v\partial_x^2 v,$$

the condition

$$k = h^2/8v \tag{3.5}$$

is necessary to provide the consistent amount of diffusion. For a system of equations, the extension of (3.5) requires that

$$k = \frac{h^2}{8v_i} = \ldots = \frac{h^2}{8v_p},$$

which is impossible to satisfy unless a different grid spacing h_i is used for each different value of v_i, such that

$$k = \frac{h_i^2}{8v_i}, \quad i = 1, 2, \ldots, p.$$

The two-point boundary value problems then can be solved on the finest grid, with boundary values interpolated at that gird. The initial values for the Riemann problems are interpolated from the solution to (3.4) on the finest grid.

The computation required in solving the large number of boundary value problems could be prohibitive. However, Sod [20] proposed the use of a dictionary. Equation (3.3) can be reduced by omitting the advection term

$$\overline{V}\partial_x^2 \boldsymbol{v} + \boldsymbol{G}(\boldsymbol{v}) = 0$$

which is independent of x and t and the solution is only needed at the midpoint. Therefore, it is necessary to consider different possibilities for the boundary values (3.4) and solution for other boundary values can be obtained by using a dictionary and linear interpolations.

B. Application to Combustion

Let $\boldsymbol{v} = (Y_A, T)$. Then, (1.2) can be written as

$$\partial_t \boldsymbol{v} + (\boldsymbol{u} \cdot \nabla)\boldsymbol{v} = \bar{\nu}\triangle \boldsymbol{v} + \boldsymbol{G}(\boldsymbol{v}) \tag{3.6}$$

where $\bar{v} = \text{diag}(Le_A^{-1}, 1)$. (3.6) is an equation of the form (3.1) except that it is not in conservation form. However, $\boldsymbol{u}$ is known at each grid point from the Navier-Stokes equation and so can be treated as a piecewise constant. The CFL condition becomes

$$\frac{k}{h} \leq \frac{1}{2\max ||\boldsymbol{u}||}.$$

In the applications, a general boundary condition is often considered:

$$a\boldsymbol{v} + c\frac{\partial \boldsymbol{v}}{\partial \boldsymbol{n}} = \boldsymbol{b}(t) \quad \text{on } \partial D, \tag{3.7}$$

where a and c are constants.

To demonstrate how the boundary conditions are implemented, without loss of generality, consider the x-sweep with $\partial D = \{x | x = 0\}$ and (3.7) becomes

$$av(0,t) + c\partial_x v(0,t) = b(t), \quad \text{on } \partial D.$$

Approximating ∂_x by a centered difference, we have

$$au_0^n + c(\frac{u_1^n - u_{-1}^n}{2h}) = b^n \tag{3.8}$$

with $t = nk, b^n = b(nk)$. The grid point corresponding to $i = -1$ lies outside the physical domain. We may solve (3.8) for u_{-1}^n

$$u_{-1}^n = u_1^n + \frac{2h}{c}(au_0^n - b^n). \tag{3.9}$$

In order to find the approximate solution at the next time level at the boundary $x = 0$, we need to establish a left and a right state for the Riemann problem associated with this point. The appropriate two-point boundary value problem is solved on the

interval [-h,0] with the left boundary condition given by (3.9), and an appropriate two-point boundary value problem is solved on the interval $[0, h]$. If $c = 0$, the solution is known at $x = 0$ and a Riemann problem is not needed at this point.

§4. A Test Problem for the Random Choice Method

For physical problems in two or more space dimensions, extenion of the random choice method requires splitting the source terms into an x-sweep followed by a y-sweep. To test the splitting of the source term, we consider

$$\partial_t v = \partial_x^2 v + \partial_y^2 v + v \tag{4.1a}$$

with initial condition

$$v(x, y, 0) = \sin(x + y) \tag{4.1b}$$

where $D = \{x, y | 0 \leq x, y \leq \pi\}$. The equation has an exact solution

$$v(x, y, t) = e^{-t} \sin(x + y). \tag{4.2}$$

In the text problem, Dirichelet boundary conditions are applied by taking values from this exact solution on ∂D.

In this case, splitting of the source term $G = v$ is required for decomposing equation (4.1a) into

$$\frac{1}{2}\partial_t v = \partial_x^2 v + \frac{1}{2} v, \tag{4.3a}$$

$$\frac{1}{2}\partial_t v = \partial_y^2 v + \frac{1}{2} v. \tag{4.3b}$$

Table 1. Maximum errors for the test of operator splitting

		Maximum errors	
Entry	Time	40×40 grid	80×80 grid
1	$t = 0.10$	6.6946E-02	3.2655E-02
2	$t = 0.20$	6.3831E-02	3.0818E-02
3	$t = 0.30$	5.7108E-02	2.9676E-02
4	$t = 0.40$	5.1835E-02	2.4805E-02
5	$t = 0.50$	4.6590E-02	2.3323E-02
6	$t = 0.60$	4.2024E-02	2.0306E-02
7	$t = 0.70$	3.7256E-02	1.8536E-02
8	$t = 0.80$	3.3752E-02	1.6625E-02

Equation (4.3a) is solved by an x-sweep and followed by a y-sweep for (4.3b). Figure 1 shows the exact and numerical solutions for $x = y$ at times $t = 0.2$ and 0.8 on a 80×80

gird. The maximum errors of the numerical solution for (4.1) are shown in Table 1. It can be seen that gird spacing is important in this application.

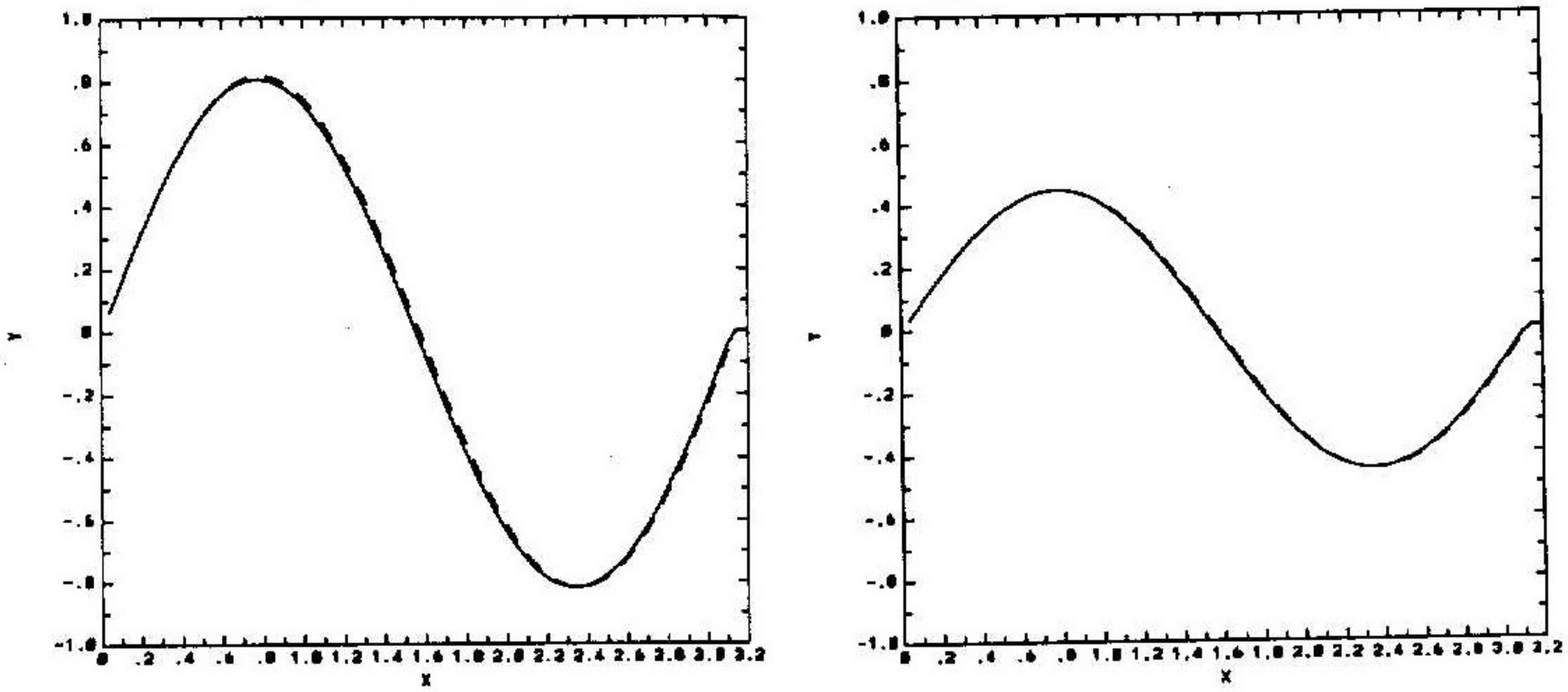

(a) $t = 0.2$ (b) $t = 0.8$

Fig. 1. Exact and numerical solutions of equation (4.1) on $x = y$

§5. Numerical Results

Consider a circular cylinder of radius 1, immersed in an incompressible gas fluid of density 1, to which is imparted at time $t = 0$ constant velocity of magnitude U_∞. We should study the development of the flow by the vortex method and the propagation of the flame in two cases: 1) the cylinder is cold; 2) the cylinder is heated.

A. Hydrodynamics

We use the hybrid vortex method for hydrodynamics. Near the boundary the computational elements are vortex sheets; outside the boundary layer we use vortex blobs. Sheets moving out of the boundary layer become blobs with $\xi_{blob} = \triangle h * \xi_{sheet}$. However, sheets which cross the boundary are reflected back to preserve the vorticity.

In Step 2 of the vortex method, potential flow can be replaced by the method of images using the circle theorem (Milne-Thomson[16]). The free stream velocity at infinity with components $(U_\infty, 0)$. The complex potential in the absence of the cylinder is $U\infty z$, and with the cylinder present becomes $\omega = U_\infty + U_\infty a^2/z$ and the stream function of this complex potential is

$$\psi(x, y) = \text{Image}\,(\omega) = -U_\infty y\Big(1 - \frac{a^2}{x^2 + y^2}\Big).$$

Then the free stream velocity (u_{pi}, v_{pi}) in (2.10) has to be modified:

$$U = \begin{cases} u_p = -\dfrac{\partial \omega}{\partial y} = U_\infty \Big[1 - \dfrac{a^2(x^2 - y^2)}{(x^2 + y^2)^2}\Big], \\ \\ v_p = -\dfrac{\partial \omega}{\partial x} = -U_\infty \Big[\dfrac{2a^2 xy}{(x^2 + y^2)^2}\Big]. \end{cases} \tag{5.1}$$

Let a point vortex of strength κ at the point $z = z_0$, for which the complex potential is $\omega = -\dfrac{i\kappa}{2\pi}\log(z - z_0)$. In the presence of the circular cylinder, the complex potential becomes $\omega = -\dfrac{i\kappa}{2\pi}\log\Big\{\dfrac{(z - z_0)z}{a^2 - z\bar{z}}\Big\}$. Since the image system consists of a point vortex of strength κ at the origin and one of strength $-\kappa$ at the point $z = a^2/\bar{z}_0$ inverse to the position of the original vortex, in the formula (2.10) (u_i, v_i) become

$$u_i = \sum_{i \neq j}{}' \frac{(y_j - y_i)}{2\pi r_{ij}^2}\xi_j + \sum_{i \neq j}{}' \frac{\Big(\dfrac{a^2 y_j}{x_j^2 + y_j^2} - y_i\Big)}{2\pi (r'_{ij})^2}\xi_j + \sum_{i \neq j}{}' \frac{-y_i}{2\pi r_{i0}^2}\xi_j$$

$$+ \sum_{i \neq j}{}'' \frac{(y_j - y_i)}{2\pi\sigma r_{ij}}\xi_j + \sum_{i \neq j}{}'' \frac{\Big(\dfrac{a^2 y_j}{x_j^2 + y_j^2} - y_i\Big)}{2\pi\sigma (r'_{ij})}\xi_j + \sum_{i \neq j}{}'' \frac{-y_i}{2\pi\sigma r_{i0}^2}\xi_j,$$

$$v_i = \sum_{i \neq j}{}' \frac{-(x_j - x_i)}{2\pi r_{ij}^2}\xi_j + \sum_{i \neq j}{}' \frac{-\Big(\dfrac{a^2 x_j}{x_j^2 + y_j^2} - x_i\Big)}{2\pi\sigma (r'_{ij})^2}\xi_j + \sum_{i \neq j}{}' \frac{x_i}{2\pi r_{i0}^2}\xi_j$$

$$+ \sum_{i \neq j}{}'' \frac{-(x_j - x_i)}{2\pi\sigma r_{ij}}\xi_j + \sum_{i \neq j}{}'' \frac{-\Big(\dfrac{a^2 x_j}{x_j^2 + y_j^2} - x_i\Big)}{2\pi\sigma (r'_{ij})}\xi_j + \sum_{i \neq j}{}'' \frac{x_i}{2\pi\sigma r_{i0}^2}\xi_j$$

where $r_{ij}^2 = (x_j - x_i)^2 + (y_j - y_i)^2$, $(r'_{ij})^2 = \Big(\dfrac{a^2 x_j}{x_j^2 + y_j^2} - x_i\Big)^2 + \Big(\dfrac{a^2 y_j}{x_j^2 + y_j^2} - y_i\Big)^2$, $r_{i0}^2 = x_i^2 + y_i^2$, Σ' is taken over $r_{ij} \geq \sigma$ and $\sum''$ over $r_{ij} \leq \sigma$.

To choose the numerical parameters, the boundary of the circle is divided into $M = 20$ pieces, each of length $\triangle h = 2\pi/M$, and cut-off σ is chosen to be $\dfrac{\triangle h}{\pi}$ (Cheer[3]). The Reynolds number is chosen from 500 to 10000. The time step size for the vortex method is chosen as $\triangle t = 0.1$.

One of the very important quantities is the drag coefficient. We use the following formula to calculate C_D (Chorin[5]):

$$C_D = C_\nu + C_p$$

where C_v is the skin drag and C_p is the form drag, given by

$$C_\nu = -\int_{\partial D} \xi_\partial \sin\theta d\theta, \quad C_p = \int_{\partial D} P_\partial \cos\theta d\theta$$

where $r\cos\theta = x$, $r\sin\theta = y$, ξ_∂ is the vorticity on ∂D and p_∂ is the pressure on ∂D;

$$P_\partial(\theta) = -\int_{\theta_0}^{\theta} \partial_n \xi ds + \text{constant}.$$

The average drag can be calculated by

$$C_D(t,T) = \int_{t-T}^{t} C_D(t)dt.$$

Figure 2 depicts the drag coefficient C_D and average drag $C_D(t,0)$ for $Re = 2000$ (marked lines A, B) and $Re = 5000$ (marked lines C, D) which are in excellent agreement with experimental values (Schlichting[17]). The drag coefficient for the Reynolds number 2000 starts at a higher value. Because of the impulsive start of the cylinder, many vortex sheets are created on the boundary. Averaging over the time from $t = 0$ to $t = 12$, we get an average drag coefficient of $C_D = 0.933$ which agrees with the experimental result very well. As we increase the Reynolds number, we find that $C_D = 1.04$ at $Re = 5000$; this rise is also experimentally observed.

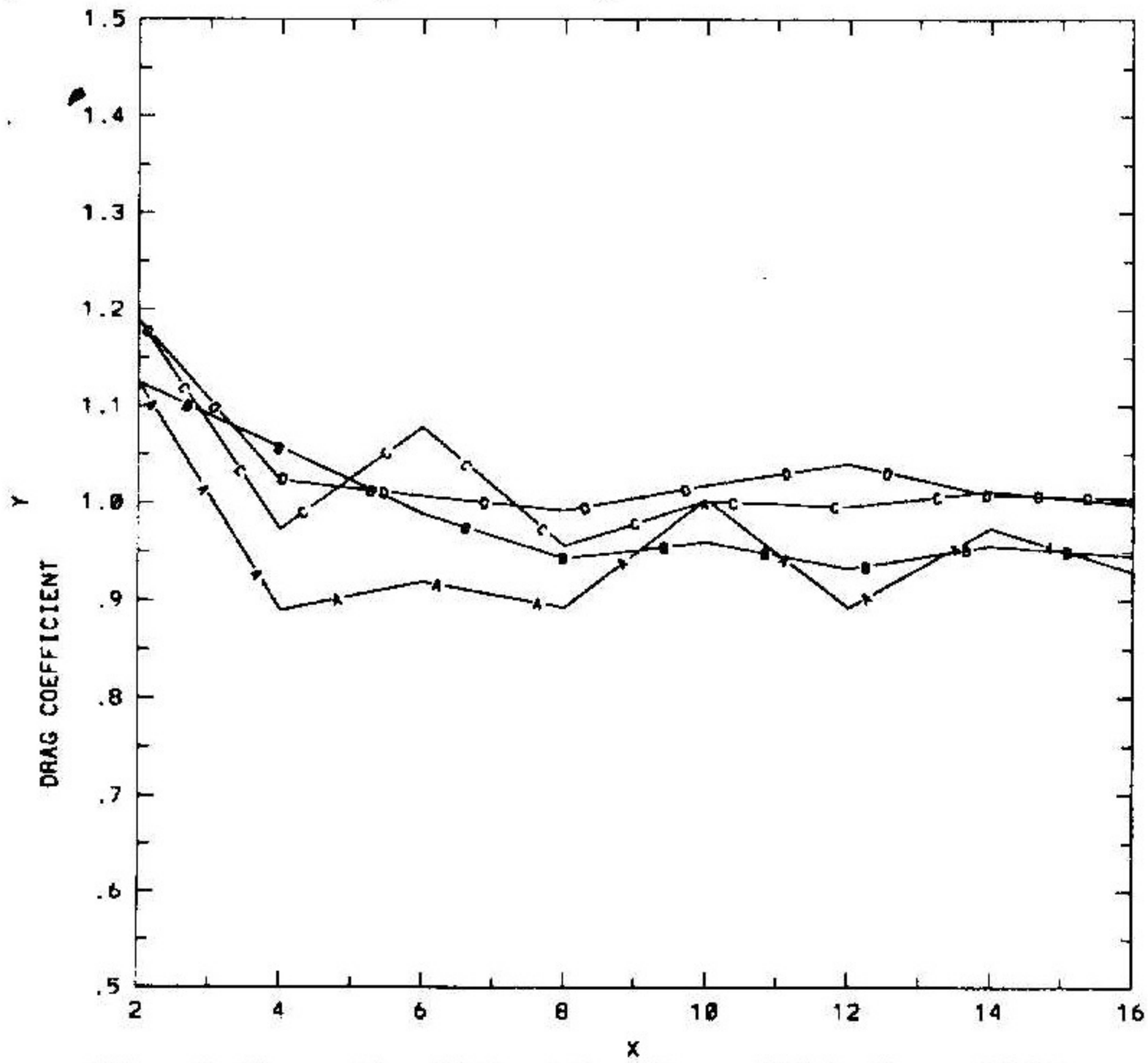

Fig. 2. Drag Coefficient for $Re = 2000, Re = 5000$
A–denote $C_D(t)$ and B–denote $C_D(t,0)$ for $Re = 2000$.
C–denote $C_D(t)$ and D–denote $C_D(t,0)$ for $Re = 5000$.

Figures 3a–d depict the velocity profile at times $t = 4.0, 6.0, 8.0$ and 10.0 for $Re = 5000$. At the early time stage, large symmetric vortices behind the circle are developed, and small vortices near the boundary are observed near the boundary due to the vorticity creation to satisfy the no-slip condition. But while this condition persists in front of the cylinder, where the fluid is accelerated, backward flow would push

the particles near the boundary into the main stream, the symmetry is lost. This has very good agreement with the experimental results (see Batchelor [2], Lewis [13]).

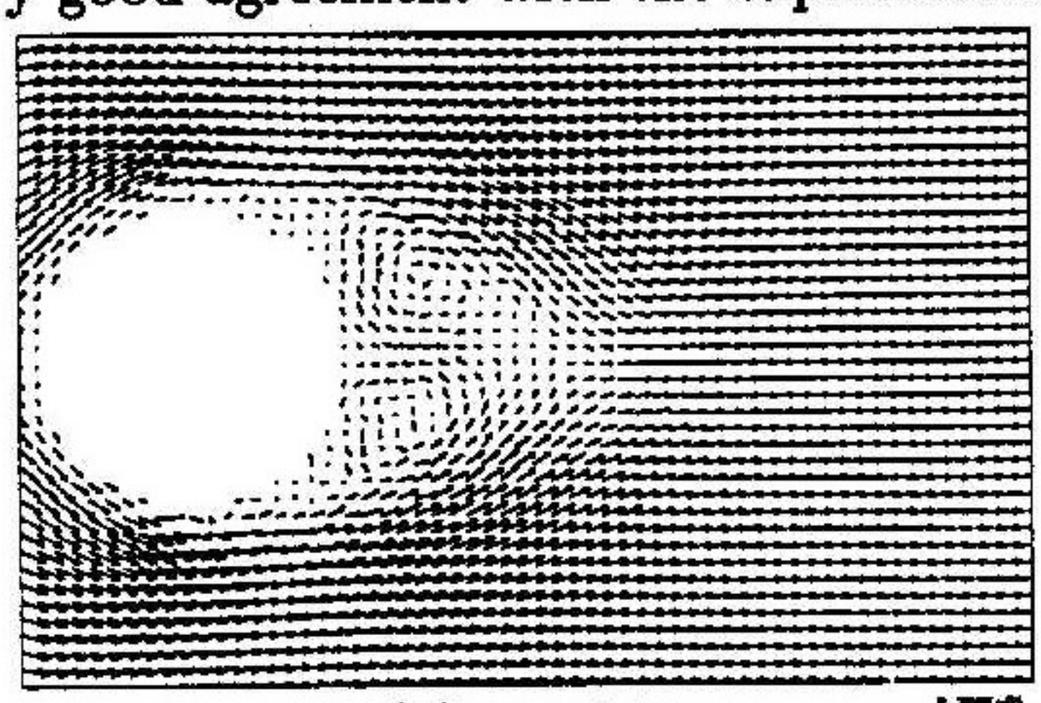

(a) $t = 4.0$

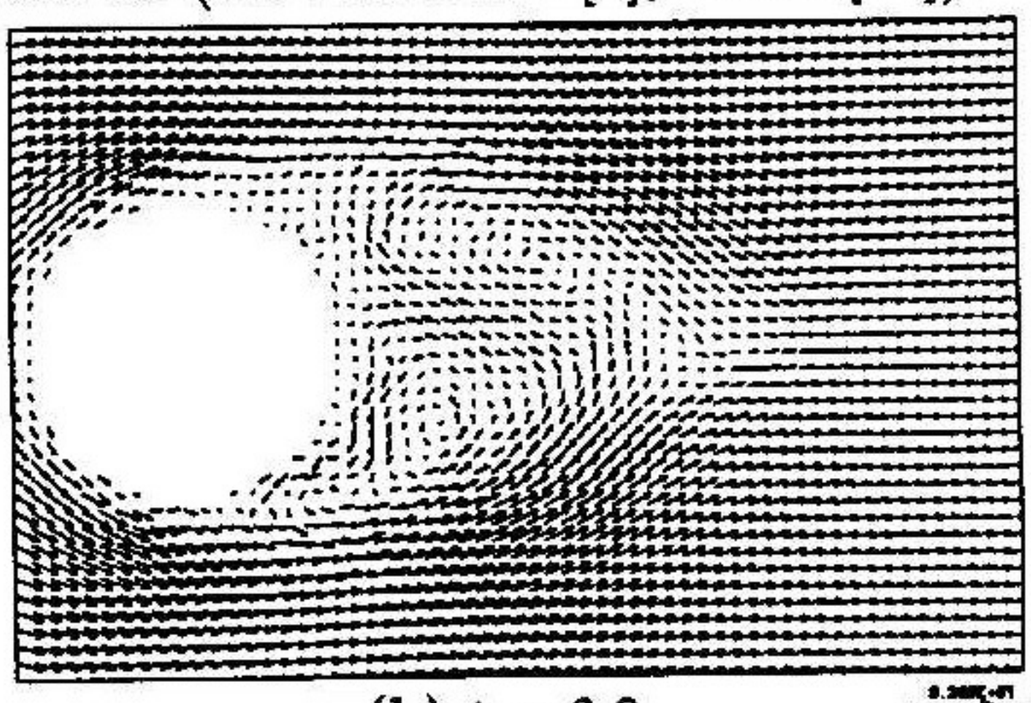

(b) $t = 6.0$

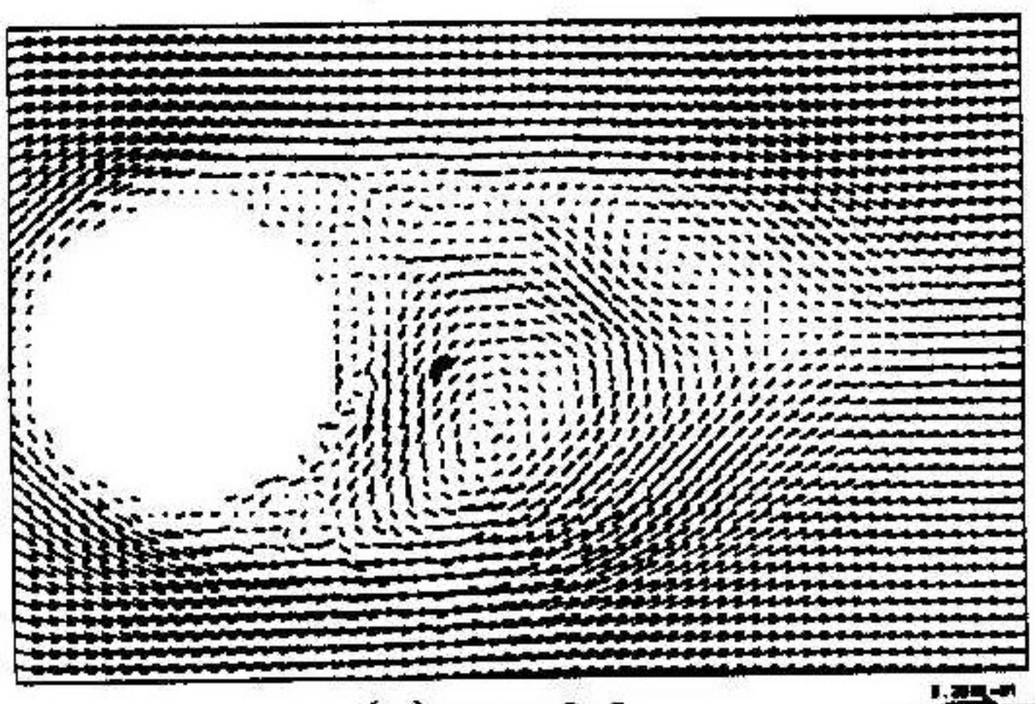

(c) $t = 8.0$

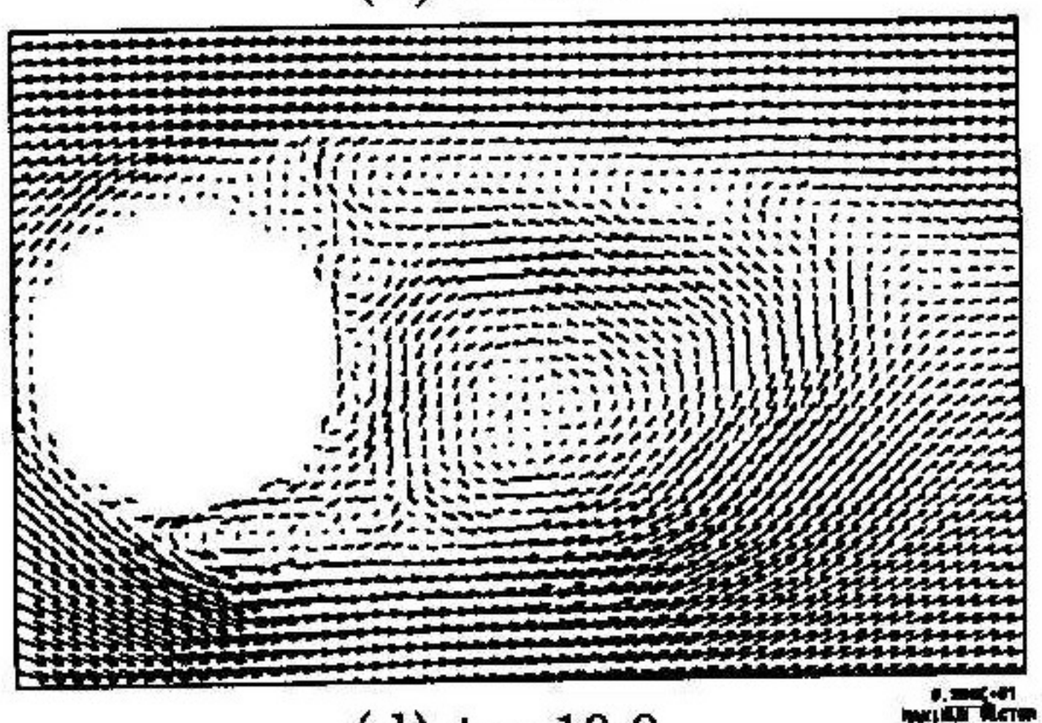

(d) $t = 10.0$

Fig. 3. Velocity Profile of flow passing a circular cylinder

B. Combustion

In our first numerical experiment of combustion, we assume that the cylinder is kept cold (ambient temperature) and the premixed gas has been ignited at $x = -\infty$ and the flame reaches the circular cylinder at $t = 0$. That gives us the following initial-boundary value problem on domain $D = \{x, y | -1.5 < x < 12, -3.0 < y < 3.0, x^2 + y^2 \geq 1\}$, with boundary conditions:

$$T = T_b, \text{ for } x = -1.5, \text{ all } y;$$

$$T = T_u, \text{ for } \partial D, \text{ i.e. } x^2 + y^2 = 1;$$

$$\partial Y_A / \partial n = 0, \text{ for all boundaries,}$$

and initial conditions

$$Y_A = 1, \text{ every where except on the circle;}$$

$$T = T_u, \text{ every where except on } x = -1.5.$$

We choose $K_A = 2.5 \times 10^3, Q_A = 1, N_A = 4, T_u = 0.2, Le_A = 1$, and grid spacing $h = 0.05$ so that the time step size is $k = 0.0003125$ by (3.5).

Flame propagation: The temperature contour profiles are compared with a) potential flow velocity (no viscosity), b) velocity calculated by the vortex method.

Figures 4a–b depict the flame profiles from case a) at times 6.0 and 10.0. Figures 5a–b depict the results from case b) at the same time levels.

In case (a), the flames move fast at earlier times, and have a very smooth flame propagation front, but the flame front can not get close to the front of the cylinder. By contrast, in case (b), the effect of vortices behind the circle is that they initially slow the burning into the front of the circle and later they help the flame front get close to the cylinder. This comparison demonstrates the importance of viscous effect in such a geometry.

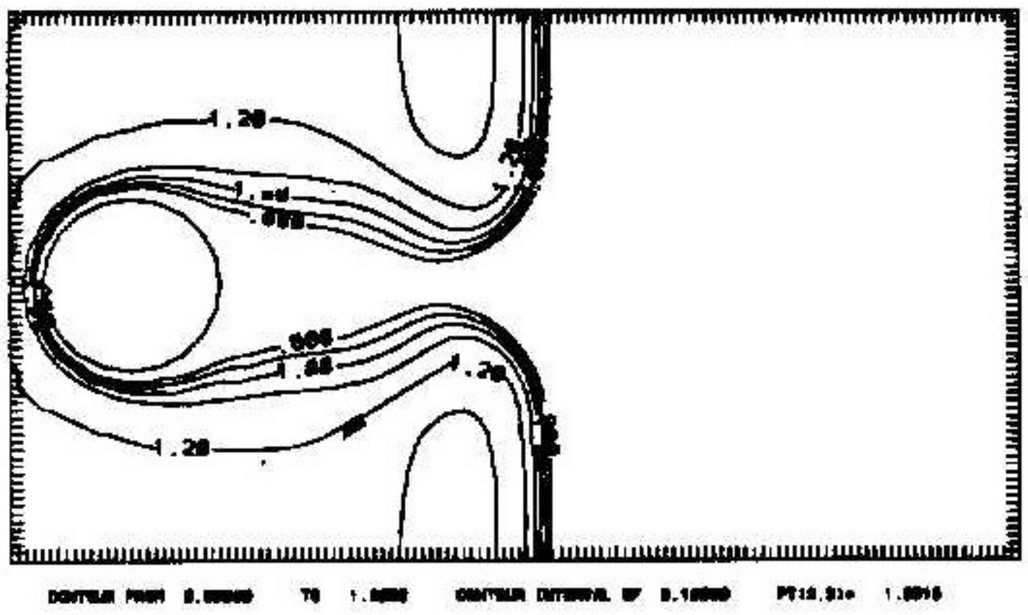

(a) $t = 6.0$

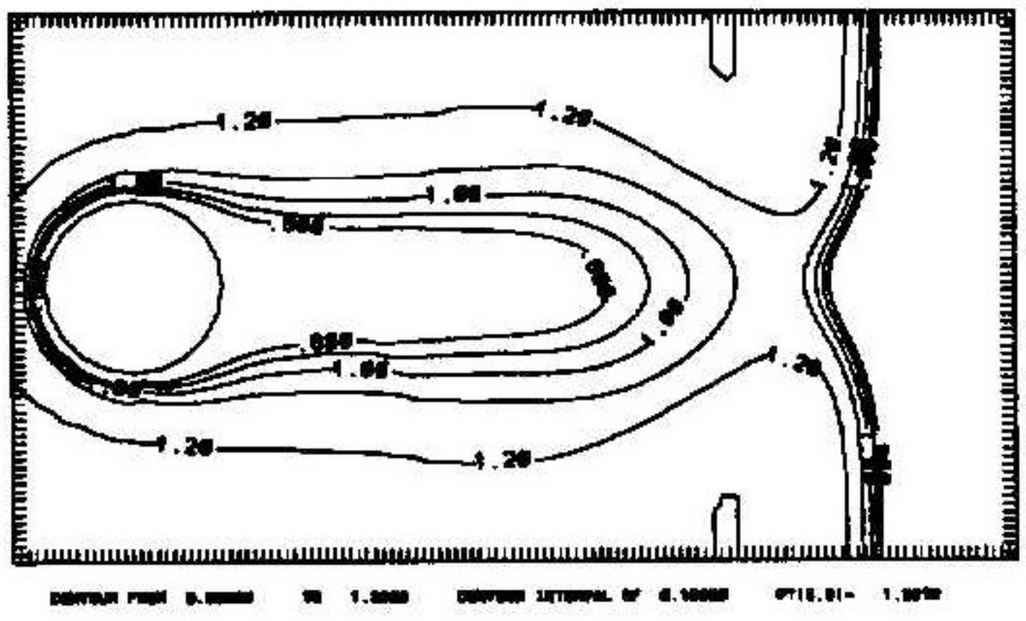

(b) $t = 10.0$

Fig 4. Flame propagation temperature contour in a cold cylinder with potential flow

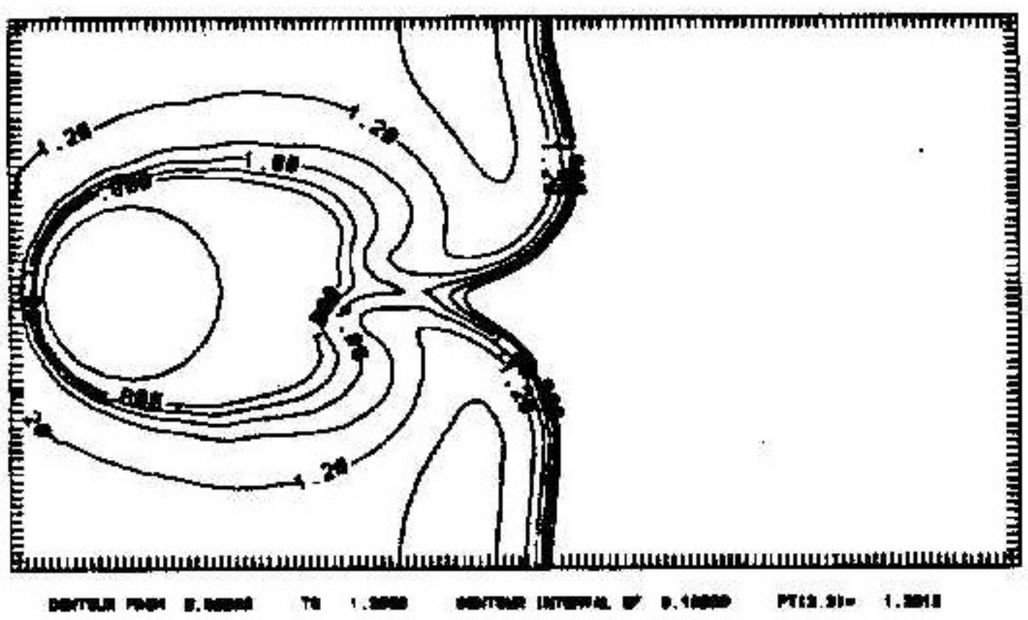

(a) $t = 6.0$

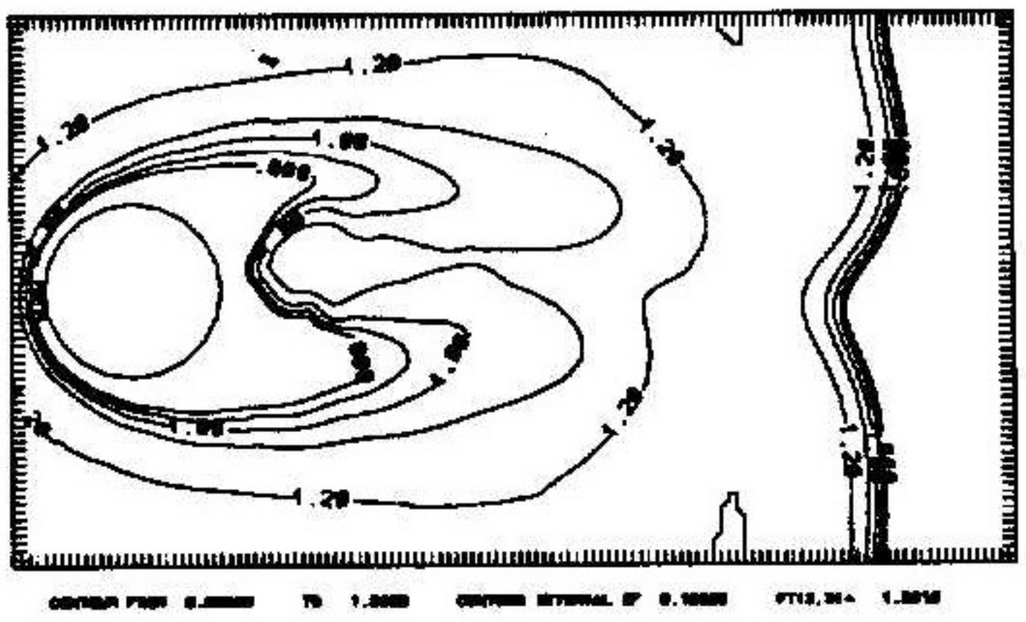

(b) $t = 10.0$

Fig 5. Flame propagation temperatire contour in a cold cylinder with the vortex method

In a systematic series of experiments, Mullen et al. [17] have studied the ignition of streams of fuel-air mixtures that pass electrically heated cylindrical rods. For the numerical study of the experiments, we consider following the initial-boundary value problem. Boundary conditions:

$$T = T_u, \text{ for } x = -2.5, \text{ all } y;$$

$$T = T_b, \text{ for } x^2 + y^2 \leq 1;$$

$$\partial Y_A / \partial_n = 0, \text{ for all boundaries.}$$

Initial conditions:

$$Y_A = 1, \text{ every where except on the cylinder;}$$

$$T = T_u, \text{ every where except on the cylinder}$$

The temperature contour profiles are compared with a) low free stream velocity: $U_\infty = 20$, and b) high free stream velocity: $U_\infty = 40$. Figure 6 depicts the flame profiles from case a) at times 4.0 and 6.0. Figure 7 depicts the results from case b) at the same time levels.

Along the surface of a hot cylinder in a cold stream, the rate of heat transfer is the largest in the two regions of maximum stream velocity where the stream is tangent to the surface.

In these regions the results show that the surface temperature is much lower than the temperature near the stagnation points.

The eddy zone behind a hot cylinder is made up partly of well-heated gas that has been in dose contact with the surface,and partly of much cooler gas that swirls back toward the cylinder from considerable a distance downstream.

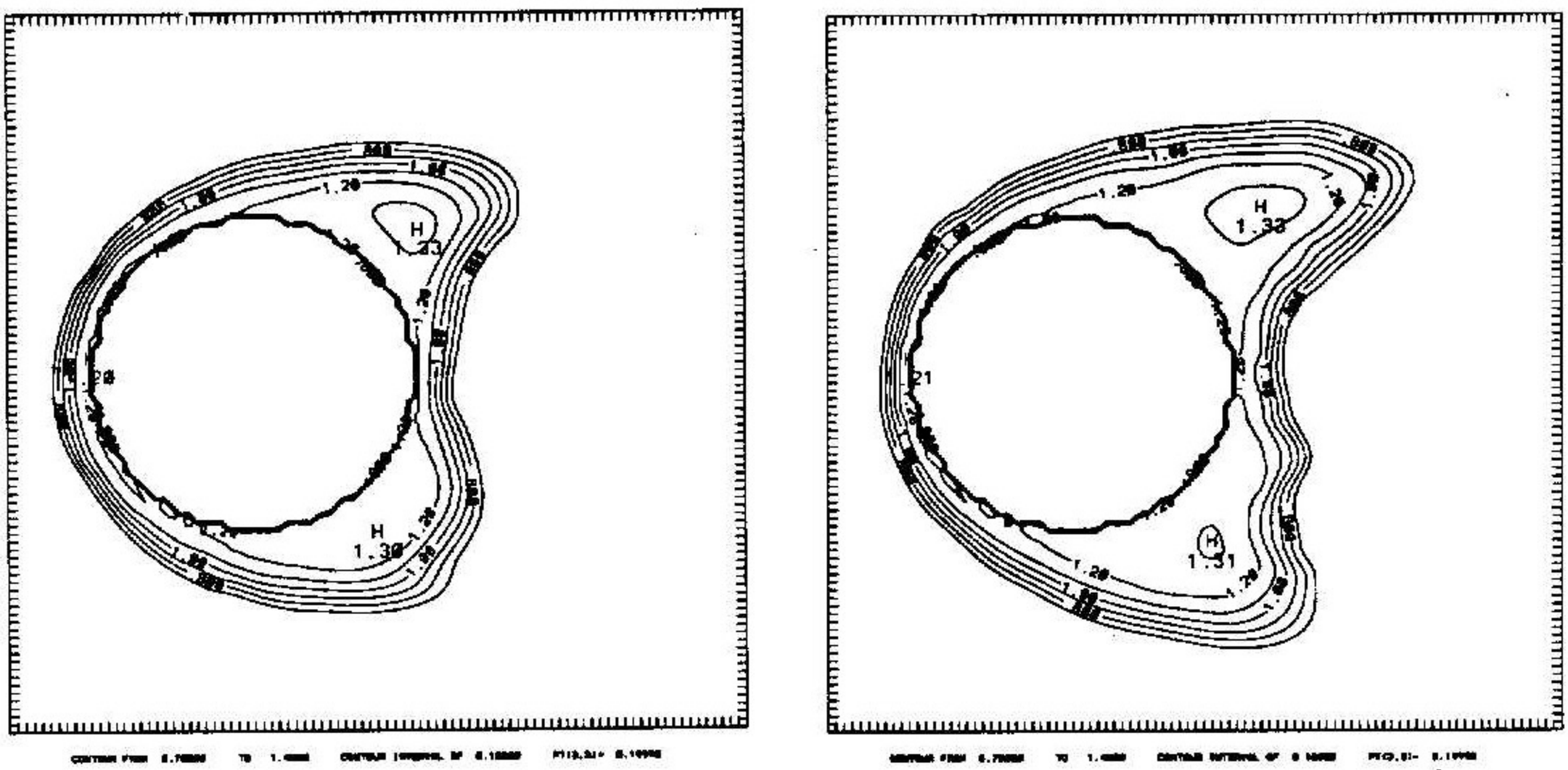

(a) $t = 4.0$ (b) $t = 6.0$

Fig. 6. Flame propagation contour with a heated cylinder at $U_\infty = 20$.

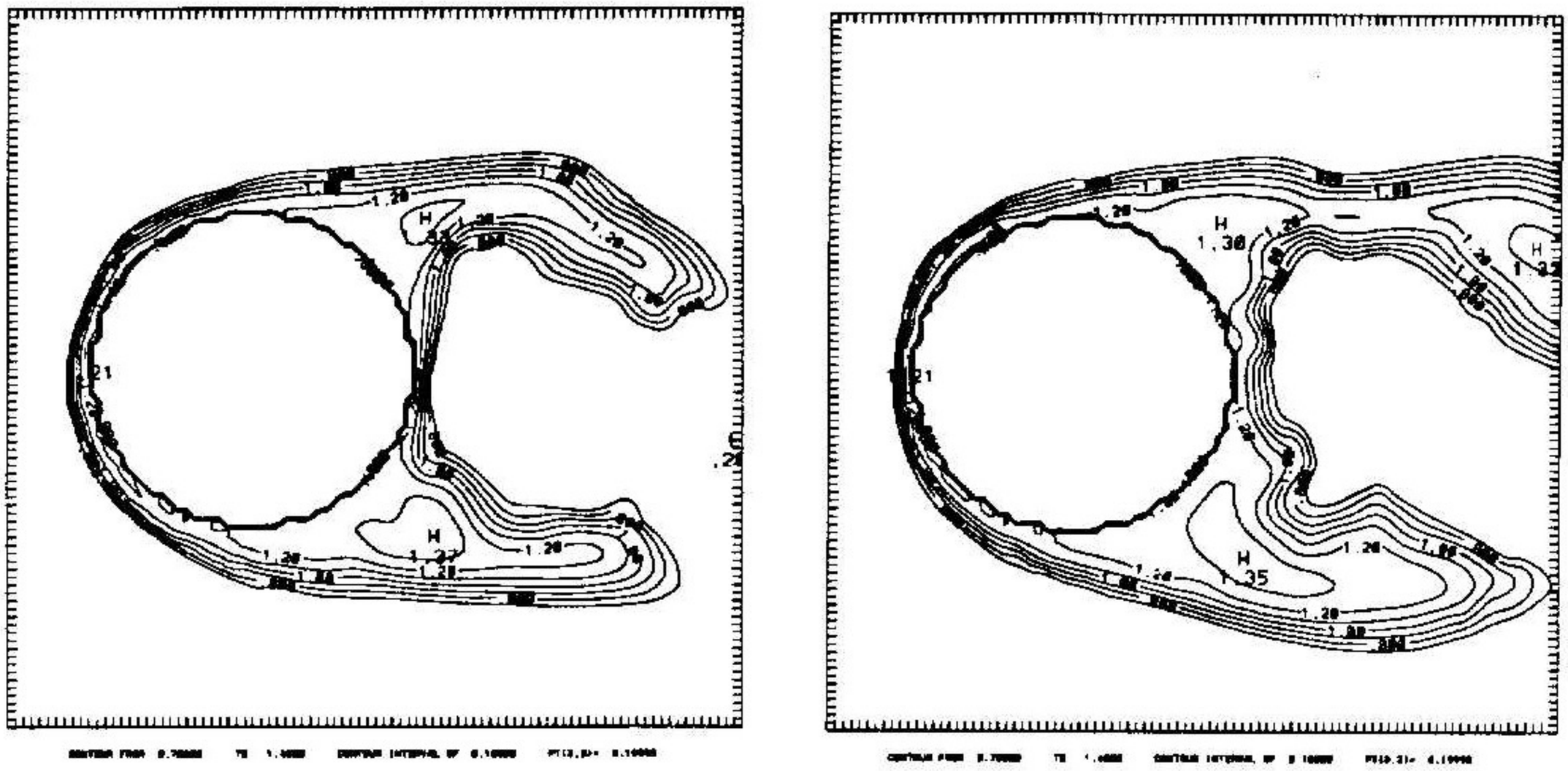

(a) $t = 4.0$ (b) $t = 6.0$

Fig. 7. Flame propagation contour with a heated cylinder at $U_\infty = 40$.

§5. Conclusions

We have presented a random numerical method. For the application in combustion of the ignition of a flow passing a circular cylinder, the desirable results were obtained. The vortices in front of the cylinder were observed to have a significant effect on the shape of the flame profiles.

The major assumption made in this model is the incompressibility of the fluid. This restricts the applicability of the method to reaction involving reactants which exhibit small thermal expansion. The next step in the improvement of this method will be to use a compressible vortex method to allow for the effects of compressibility and to solve reaction-diffusion equations involving temperature and species densities where total density is no longer constant.

There also exists a possibility of extending this model to three dimensional flows, with appropriate modification on the random vortex method (Anderson [1], Chorin [9]).

Acknowledgments. This work is part of the author's Ph.D dissertation. The author wishes to thank his advisor, Professor Gary A. Sod, for his many helpful discussions and comments.

References

[1] C.Anderson, A method for local corrections for computing the velocity field held due to a distribution of vortex blobs, *J. Comp. Phys.*, 62 (1986), 111–123.

[2] G. K. Batchelor, An Introduction to Fluid Dynamics, Cambridge University Press, Cambridge, 1967.

[3] A. Y. Cheer, Numerical study of incompressible sligtly viscous flow past blunt bodies and airfoils, *SIAM J. Sci. Stat. Comp.*, 4 (1983), 81–92.

[4] A. Y. Cheer, Unsteady separated wake behind an impulsively started cylinder in slightly viscous fluid, *J. Fluid Mech.*, 201 (1989), 485.

[5] A. J. Chorin, Numerical study of slightly viscous flow, *J. Fluid Mech.*, 57 (1973), 785–796.

[6] A. J. Chorin, Random choice solution of hyperbolic system, *J. Comp. Phys.*, 22 (1976), 517–533.

[7] A. J. Chorin, Random choice methods with application to reacting gas flow, *J. Comp. Phys.*, 25 (1977), 253–272 .

[8] A. J. Chorin, Vortex sheet approximation of boundary layer, *J. Comp. Phys.*, 27 (1978), 428–442.

[9] A. J. Chorin, Vortex models and boundary layer instability, *SIAM J. Sci. Stat. Comp.*, 1 (1980), 1–21.

[10] P.Colella, Glimm's method for gas dynamics, *SIAM J. Sci. Comp.*, 3 (1982), 76–110.

[11] R. A. Dwyer and G. R. Otey, A numerical study of the interaction of fast chemistry and diffusion, *AIAA J.*, 7 (1979), 606–617.

[12] J. Glimm, Solution in large for nonlinear hyperbolic systems of equations, *Comm. Pure and appl. Math.*, 18 (1965), 697–715.

[13] B. Lewis and G. von Elbe, Combustion, Flames and Explosions of Gases, Third Edition, Academic Press, 1987.

[14] T. P. Liu, Quasilinear hyperbolic systems, *Comm. Math. Phys.*, 68 (1979), 141.

[15] T. P. Liu, Nonliear stability and instability of transonic gas flow through a nozzle, *Comm. Math. Phys.*, 83 (1982), 243.

[16] L. M. Mile-Thomson, Theoretical Hydrodynamics, 5th Ed. MacMillian, 1968.

[17] J. M. Mullen, J. B. Fenn and M. R. Trby, Third Symposium on Combustion and Flame and Explosion Phenomena, 317, Williams & Wilkins, Baltmore 1949.

[18] H. Schlichting, Boundary Layer Theory, 7th Ed. McGra–Hill, 1979.

[19] G. A. Sod, Numerical study of converging cylindrical shock, *J. Fluid Mech.*, 83 (1977), 785–794.

[20] G. A. Sod, A flame dictionary approach to modeling unsteady combustion phenomena, *Math. Appl. Comp.*, 3 (1984), 157–182.

[21] G. A. Sod, Numerical Methods in Fluid Dynamics, Cambridge Univ. Press, 1985.

[22] G. A. Sod, A random choice method with application to reaction-diffusion system in combustion, *Int. J. Comput. and Maths. with Appl.*, 11 (1985), 129–144.

[23] G. A. Sod, A dictionary approach to reaction-diffusion systems with nonlinear diffusion coefficients, *Int. J. Comput. and Maths. with Applic.*, 13 (1987), 771–783.

[24] G. A. Sod, A random choice method for the stefan problem, *Int. J. Comput. and Maths. with appl.*, 19 (1990), 1–9.